

MERS-CoV from Africa are limited. We previously reported that MERS-CoV from Egypt and Nigeria appear to be phylogenetically distinct from those currently circulating in the Arabian Peninsula (5, 6). We now report a comprehensive genetic and phenotypic analysis of MERS-CoV from North (Morocco), West (Nigeria, Burkina Faso), and East (Ethiopia) Africa compared with viruses from the Arabian Peninsula.

Results

Genetic Characterization. The epidemiological aspects of field studies of dromedary camels in Morocco, Burkina Faso, Ethiopia, and Nigeria, including seroprevalence and RT-PCR detection of virus from nasal swabs, have been reported previously (6, 7). An additional 102 nasal swabs were collected in the Afar region of Ethiopia in 2017. Of 173 RT-PCR-positive specimens detected in these studies, those with high viral load were selected, attempting to maximize diversity in geography and sampling dates, for full viral genome sequencing directly from the clinical specimen and for virus isolation (Dataset S1). Three viruses from Burkina Faso, one from Morocco, nine from Nigeria, and three from Ethiopia were fully sequenced, and an additional virus from Ethiopia was sequenced from the S2 gene region to the 3' end of the genome (5,126 nt). Genetic nucleotide identity was 99.17% within African camel virus genomes, >99.26% within human and camel MERS-CoV from the Middle East, and 99.18–99.58% between viruses from the Middle East and Africa (GenBank accession nos: [MG923465–MG923481](#)).

Phylogenetic analysis of these and other relevant viruses is shown in Fig. 1. The tree was rooted against a MERS-CoV-related bat coronavirus Neoromicia/PML-PHE/RSA/2011 (8). Viruses from Nigeria, Burkina Faso, Morocco, and Ethiopia formed a monophyletic clade together with previously sequenced viruses from Egypt, which we now provisionally designate as virus “clade C.” A time-resolved phylogeny of currently available MERS-CoV sequences, including those generated in this study from diverse parts of Africa, is shown in Fig. S1. An analysis of synapomorphies (mutations inferred to have occurred once in

the tree), homoplasies (repeat mutations), and reversions within available MERS-CoV full-genome sequences is shown in Fig. S2. Viruses from Burkina Faso ($n = 3$), Morocco ($n = 1$), and Nigeria ($n = 9$) had signature deletions in the *ORF4b* and/or *ORF3* gene regions (Fig. S3) and are designated “clade C1” (Fig. 1). Clade C viruses from Ethiopia ($n = 4$) and Egypt ($n = 3$) did not have such gene deletions, nor do the majority of viruses from the Arabian Peninsula. However, sequences of two clade B human viruses detected in 2012 (Riyadh_1_2012 and Bisha_1_2012) available in public databases also have short (17-nt) deletions in the *ORF4b* region in a similar, although not identical, region as the African isolates (Fig. S3). Targeted sequencing of the *ORF3/4b* gene region was done on additional African camel viruses from which full genomes could not be obtained because viral load was too low. Overall, all 10 additional viruses from Burkina Faso carried these same signature deletions, frame shift mutations, or premature stop-codons that markedly reduced the size of the *ORF4b*, but none of the 10 additional viruses from Ethiopia did so (Fig. S3). Clade C1 viruses with *ORF4b* deletions appear to share a common ancestor, with a 6-nt and a 360-nt deletion in *ORF4b* denoted as the “ancestral type i *ORF4b* deletion” in the phylogenetic tree (Fig. 1) and in the schematic (Fig. S3). This deletion has been added to progressively, and these deletions are denoted as “ii,” “iii,” “iv,” and “v” along the branches of the phylogenetic tree (Fig. 1) and the schematic (Fig. S3). Some of these viruses (Nigeria/HKU NV1657-like and Burkina Faso/CIRAD-HKU697-like) have also acquired deletions in *ORF3*. Notably, the Ethiopian and Egyptian viruses encoded a full-length *ORF3*.

The impact of the different *ORF4b* deletion events on the functional domains of the putative protein are shown in Fig. S4. The type i/v deletion found in BF785 and BF434 viruses truncated the ORF4b protein from 246 aa found in the EMC prototype MERS-CoV EMC to 14 aa, deleting the whole of the nuclear localization signal as well as the enzymatic domain that cleaves 2',5'-oligoadenylate (9). Nig1657 retains the nuclear localization signal and part of the phosphodiesterase (PDE) domain and is truncated to 71 aa. All these deletions disrupt the PDE

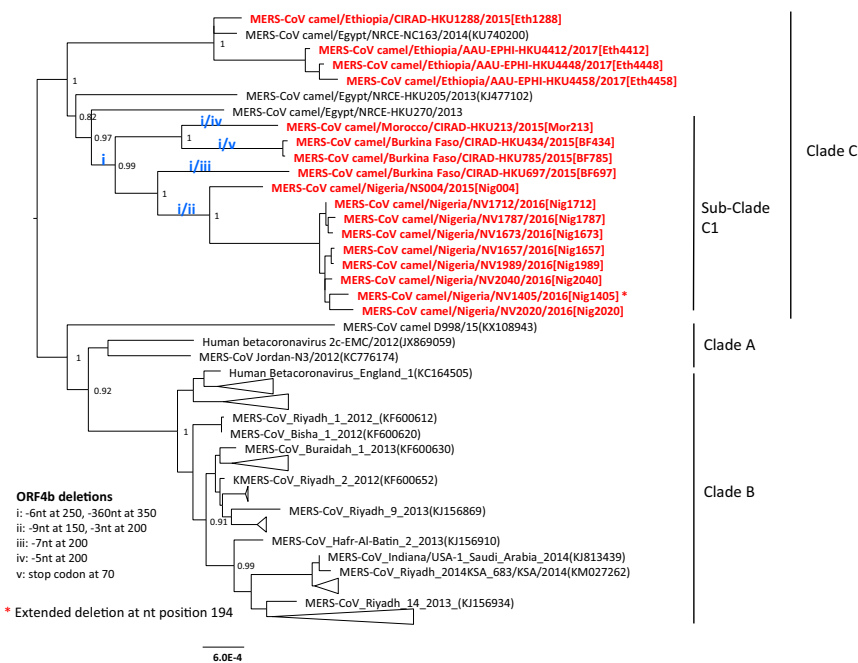


Fig. 1. Phylogenetic analysis of MERS-CoV full and partial genomes using the maximum-likelihood method (PhyML). Posterior probabilities of nodes with values higher than 0.8 are shown. The tree is rooted against a MERS-CoV-related bat coronavirus Neoromicia/PML-PHE/RSA/2011 (GenBank accession no. [KC869678](#)). The long branch leading to Neoromicia/PML-PHE/RSA/2011 has been removed to allow greater resolution of the viruses of interest. Fourteen virus genomes from African camels from this study are highlighted in red, and abbreviations for the viruses are given in square brackets. Clade C and subclade C1 MERS-CoV from African camels are denoted. Five deletion events (i–v) for viruses in clade C1 deduced from the deletion patterns affecting *ORF3* and *ORF4b* (Fig. S3) are indicated at the respective branches.

catalytic site. ORF4b encoded a polypeptide known to be an IFN antagonist (10, 11). The N-terminal region of ORF4b encodes the nuclear localization signal. Deletion of this region abrogated nuclear localization and led to a loss of suppression of IFN- β induction via the IRF3- and IRF7-signaling pathways. However, it did not affect suppression of IFN- β via Tank-binding kinase 1 and I κ B kinase, which was demonstrated in transient transfection experiments and appears to be mediated by the C-terminal domain of ORF4b (10). These data come from ORF4b protein overexpression and may or may not be physiologically relevant. The two Saudi Arabian clade B viruses Riyadh_1 and Bisha_1 had less extensive deletions of the PDE domain, although they also disrupt the PDE catalytic site.

Deletions and insertions at the 3' end of *ORF3* from viruses from Nigeria (including Nig1657) and five viruses from Burkina Faso (BF697, BF698, BF748, BF750, and BF764) resulted in the truncation of the 103-aa ORF3 polypeptide to 98, 88, or 84 aa (Fig. S3). The *ORF3* deletions occurred only in those viruses from Nigeria with type i/ii *ORF4b* deletions and in some viruses from Burkina Faso with type i/iii *ORF4b* deletions. These deletions occurred near the 3' end of *ORF4b* and *ORF3* and did not affect the integrity of transcription regulator sequences (12) of downstream genes. They are therefore unlikely to affect the transcription of subgenomic RNAs.

The amino acid residues of AH13, Nig1657, and BF785 that differ from the prototype clade A MERS-CoV strain EMC occur throughout the virus genome (Dataset S2). The amino acid sequence of the Egyptian virus NRCE-HKU270, an East African virus most closely related to the West African clade C1 viruses, is also included for comparison. The amino acid residues in the receptor-binding domain of the spike proteins of the BF785 had amino acid substitution T424I, while Nig1657 had amino acid substitutions L495F and L588F. None of these amino acid substitutions was at the receptor-interacting interface of the spike protein and thus likely did not affect the affinity of the protein for the host receptor, although L495F is close to the interacting interface.

The antigenic similarity of BF785 and Nig1657 was compared with prototype strain EMC, AH13, and Egypt NRCE-HKU270 by microneutralization tests using serum from a dromedary camel immunized with a vaccinia-vectored MERS-CoV strain EMC spike vaccine (provided by B. L. Haagmans, Erasmus University Medical Center, Rotterdam) (13) and two field-collected dromedary camel sera from Saudi Arabia (Table S1). Each serum neutralized all MERS-CoV to titer dilutions twofold or less than observed with prototype virus EMC.

Phenotypic Characterization. Three viruses from Burkina Faso and one from Nigeria were successfully isolated in cell culture, *viz.*, dromedary/Burkina Faso/CIRAD-HKU434/2015 [BF434], dromedary/Burkina Faso/CIRAD-HKU482/2015 [BF482], dromedary/Burkina Faso/CIRAD-HKU785/2015 [BF785], and dromedary/Nigeria/HKU NV1657 [Nig1657]. A representative dromedary virus, BF785, with *ORF4b* deletion type i/v, the most extensive deletion of *ORF4b* without any *ORF3* indel, and Nig1657, with partial deletion of *ORF4b* (type i/ii) together with an *ORF3* deletion, were selected for detailed phenotypic characterization. We confirmed that the limited passage of virus isolates in cell culture had not extended the ORF deletions observed in direct sequences from the specimen. These viruses were compared with the prototype MERS-CoV EMC strain (clade A) and a dromedary virus isolated in the Kingdom of Saudi Arabia AH13 (clade B). Neither EMC nor AH13 has truncations in *ORF4b* or *ORF3*.

Calu-3 cells, a human adenocarcinoma cell line of bronchial epithelial origin that retains innate immune function, were infected at a multiplicity of infection (MOI) of 0.01. EMC and AH13 strains replicated comparably with each other, while BF785 and Nig1657 replicated to significantly lower titer at 24 and 48 h postinfection (Fig. 2A) and area-under-curve (AUC) analysis (Fig. S5A). Similar observations were made in Calu-3 cells infected at an MOI of 0.1 with EMC, AH13, and BF785 viruses (Fig. S5B and C). In experimentally infected

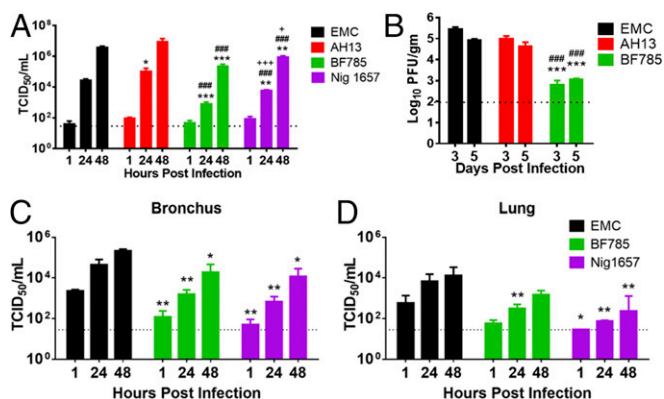


Fig. 2. Comparison of virus replication kinetics in Calu-3 cells, human DPP4-transduced mice, and ex vivo cultures of the human bronchus and lung. (A) Calu-3 cells were infected at an MOI of 0.01, and virus titers in culture supernatants were determined by the 50% tissue culture infective dose per milliliter (TCID₅₀) assay. The horizontal dotted line denotes the limit of detection in the TCID₅₀ assay. Statistical significance was determined by two-way ANOVA with Bonferroni's correction: **P* < 0.05; ***P* < 0.01; ****P* < 0.001 compared with EMC; ####, *P* < 0.001 compared with AH13; +, *P* < 0.05; ++, *P* < 0.001 compared with BF785. Each experiment was repeated once, and one representative experiment is shown. (B) Ad5-hDPP4-transduced C57BL/6 mice (7 wk old, female) were infected intranasally with 1×10^4 pfu of MERS-CoV strains EMC, AH13, or BF785. Virus titers in the lungs were measured. The horizontal dotted line denotes the limit of detection. Titers are expressed as pfu per gram of tissue. *n* = 3 mice per group at each time point. Statistical significance was determined by two-way ANOVA with Bonferroni's comparisons: ****P* < 0.001 compared with EMC; ####, *P* < 0.001 compared with AH13. (C and D) Comparison of virus replication and tropism of MERS-CoV EMC, BF785, and Nig1657 in ex vivo cultures of human bronchus (C) and lung (D). Virus titers in culture supernatants were determined by TCID₅₀ assay. Data are the means and SEM of three individual tissue donors. The horizontal dotted line denotes the limit of detection in the TCID₅₀ assay. Statistical significance was determined by two-way ANOVA with Bonferroni's comparisons: **P* < 0.05; ***P* < 0.01 compared with EMC.

C57BL/6 mice made susceptible to infection with MERS-CoV by transducing the human dipeptidyl peptidase receptor (hDPP4) using an adenovirus type 5 vector expressing hDPP4 (14), BF785 viral titers in the lung were significantly lower than EMC or AH13 virus titers at both day 3 and day 5 post infection, the difference in viral titers being $>2\log_{10}$ at 3 d post infection (Fig. 2B), although histology did not reveal obvious differences in pathology (Fig. S6). MERS-CoV BF785 and Nig1657 replicated less efficiently than EMC in ex vivo cultures (15) of human bronchus and lung (Fig. 2C; Fig. S5D shows the AUC). The immunohistochemistry of infected human bronchus and lung did not reveal any obvious difference in tropism (Fig. S5E).

A genetic feature observed in BF785 and Nig1657 was the deletion in *ORF4b*. *ORF4b* gives rise to a gene product that is reportedly associated with evasion of host cell IFN defense mechanisms (10, 11), and these deletions would be expected to impact *ORF4b* function. We therefore compared innate immune responses elicited in Calu-3 cells by infection with EMC, AH13, BF785 (which has most of its *ORF4b* gene deleted), and Nig1657 (which has *ORF4b* partially deleted as well as an *ORF3* deletion) viruses after infection at an MOI of 2 (Fig. 3). A highly pathogenic avian influenza virus, A/HK/483/1995 (H5N1), was used as a positive control of cytokine and IFN-stimulated gene (ISG) expression. UpE gene expression in MERS-CoV-infected cells confirmed that BF785 and Nig1657 had lower replication than EMC and AH13 (Fig. 3A). IFN- β , IFN- λ 1/IL-29, IP-10 (CXCL10), ISG15, and Mx1 mRNA expression was strongly up-regulated as early as 24 h post infection in H5N1-infected cells, at which time there was minimal induction of these genes in MERS-CoV-infected cells (Fig. 3B–G). By 48 h after infection IFN- β , IFN- λ 1/IL-29, IP10 (CXCL10), ISG15, MX1, and TNF- α mRNA was detectable in cells infected with all

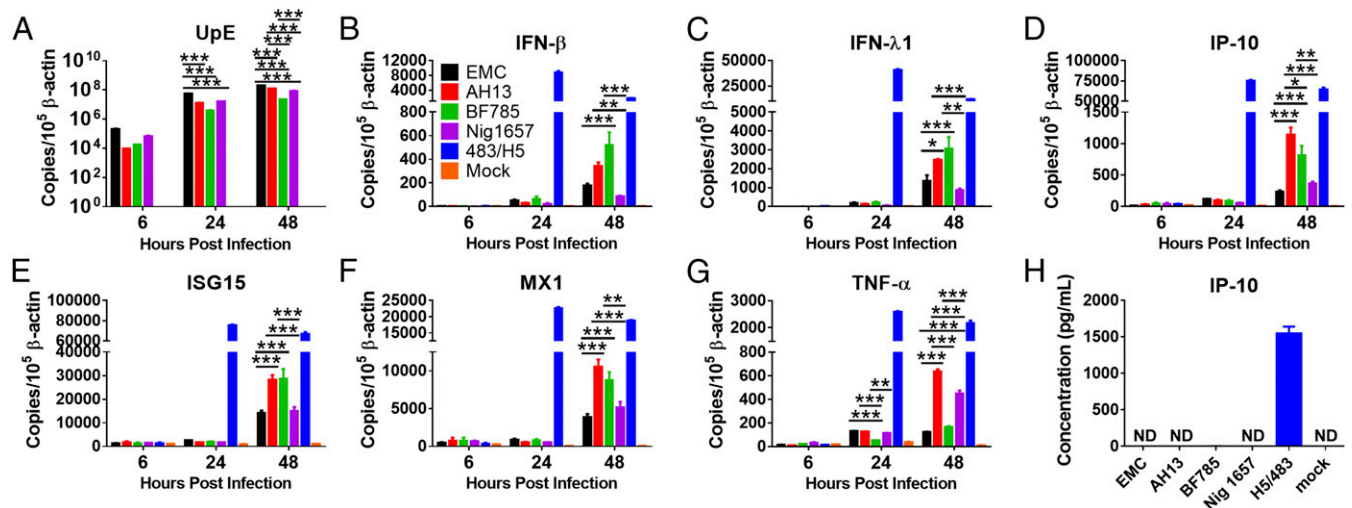


Fig. 3. Comparison of innate immune responses in Calu-3 cells infected with different MERS-CoVs: EMC, AH13, BF785, or Nig1657. Calu-3 cells were infected with MERS-CoV at an MOI of 2. Influenza A/HK/483/1997 (H5N1) was used as a positive control for cytokine induction, and mock-infected cells served as negative controls. Cell lysates were collected at 6, 24, and 48 h postinfection, and mRNA was extracted. The RNA expression of viral gene (UpE) (A), mRNA expression of IFNs (IFN- β , and IFN- λ 1) (B and C), IFN-inducible genes IP-10 (D), ISG15 (E), and MX1 (F), and a proinflammatory cytokine TNF- α (G) is shown as the mean and SEM of three biological replicates. The detection limit of each gene was 20 copies. (H) The cell-culture supernatants were tested for IP-10 protein using the BD Cytometric bead-assay (detection limit 7.54 pg/mL). The experiment was carried out with three biological replicates. Statistical significance was determined by two-way ANOVA with Bonferroni's correction and is indicated as * $P < 0.05$; ** $P < 0.01$; *** $P < 0.001$.

four MERS-CoV isolates, but levels remained markedly lower than in H5N1-infected cells. IFN- β , IFN- λ 1/IL-29, and IP-10 (CXCL-10) mRNA in BF785-infected cells was significantly higher than that seen in EMC but was not higher than in AH13-infected cells. Nig1657-infected cells had significantly lower levels of IFN- β , IFN- λ 1/IL-29, IP10 (CXCL-10), ISG15, and MX1 mRNA compared with AH13- or BF785-infected cells (Fig. 3 B–F). IP-10 (CXCL10) protein levels in the supernatants of the four MERS-CoV-infected cells were below the limits of detection or were very low compared with H5N1-infected cells (Fig. 3H). We also investigated the sensitivity of the four MERS-CoV to increasing concentrations of IFN- β in Vero cells and found no biologically relevant difference between the Saudi Arabian and African viruses (Fig. S7). All four MERS-CoV were markedly more sensitive to IFN- β than has been reported for Severe acute respiratory syndrome coronavirus (SARS-CoV) (16).

Phenotype of Δ ORF4b EMC Virus. To directly address whether the *ORF4b* deletion affects viral replication competence, we used reverse genetics to derive a recombinant EMC virus carrying the *ORF4b* deletion (rgEMC Δ 4b) and compared this with an isogenic recombinant wild-type virus (rgEMC-WT). Replication competence of rgEMC Δ 4b virus in Calu-3 cells infected at an MOI of 0.01 was not significantly different from rgEMC-WT virus as assessed by infectious virus titers at 24 h post infection, although it was reduced at 48 and 72 h post infection (Fig. 4A). In Calu-3 cells infected at an MOI of 2.0, viral UpE gene expression was comparable or lower in rgEMC Δ 4b-infected cells (Fig. 4B), but the expression of IFN- β , IFN- λ 1/IL-29, CXCL10 (IP-10), ISG15, Mx1, and TNF- α was significantly higher (Fig. 4C and Fig. S8).

Discussion

Studies of MERS-CoV in dromedaries in Burkina Faso (West Africa), Nigeria (West Africa), Morocco (North Africa), and Ethiopia (East Africa) showed that virus circulation was as extensive and viral shedding as common as previously reported in the Arabian Peninsula (7). However, while zoonotic MERS has been repeatedly reported from the Arabian Peninsula, zoonotic human disease has not so far been reported in Africa. There are, however, little viral genetic data from MERS-CoV in Africa. To begin to address this knowledge gap, we genetically characterized MERS-CoV from Burkina Faso, Nigeria, Morocco, and Ethiopia. We

found that MERS-CoV circulating in dromedaries in Africa are phylogenetically distinct from viruses in the Arabian Peninsula. There are no homoplasies (convergent mutations) shared between the African and Saudi clades, suggesting no recombination between these lineages (consistent with a single or just a few introductions into the Kingdom of Saudi Arabia and limited further contact between the lineages). MERS-CoV from North and West Africa form a distinct subclade (clade C1) within those from Africa, and they have characteristic deletions in *ORF4b*, an accessory gene that has been previously reported to be an IFN antagonist (10, 11). Some of these viruses also have partial deletions of *ORF3*. The biological function of *ORF3* still remains unclear. Dromedary camel movements in Africa occur more in the north-south direction with movements between countries such as Morocco, Burkina Faso, and Nigeria being more much likely than east-west movements, i.e., between West Africa and Ethiopia or Egypt (17). This may explain the observed separate phylogenetic clustering of viruses from West and North Africa as clade C1, which were also the viruses that have the *ORF4b* gene deletions. Although genetically distinct, MERS-CoV from West Africa were antigenically similar to the prototype EMC virus (clade A), AH13 (clade B), and Egypt NRCE-HKU270 (clade C, nonclade C1) viruses in microneutralization tests. Thus, it is likely that neutralizing antibodies elicited by the prototype strain EMC in putative vaccines are likely to be cross-protective against these genetically diverse African strains.

We successfully isolated representative clade C1 viruses from West Africa (BF785 from Burkina Faso and Nig1657 from Nigeria) for phenotypic characterization in comparison with human clade A (strain EMC) virus and a camel clade B (AH13) virus from Saudi Arabia. BF785 has the most extensive deletion of the *ORF4b* gene product, with loss of the whole PDE domain as well as the nuclear-localizing signal, while Nig1657 retains the nuclear-localizing domain and part of its PDE domain, although the PDE catalytic site is lost. Compared with EMC and AH13, both BF785 and Nig1657 viruses had significantly reduced replication competence in Calu-3 cells as assessed by titration of infectious virus at 24 and 48 h post infection at MOIs of 0.01 and 0.1, respectively. In contrast, we had previously demonstrated that the East African dromedary/Egypt-NRCE-HKU-270/2013 had comparable or better replication competence than EMC and AH13 viruses in Calu-3 cells (15). Compared with EMC and AH13, the BF785 virus also had reduced replication competence *in vivo* in the

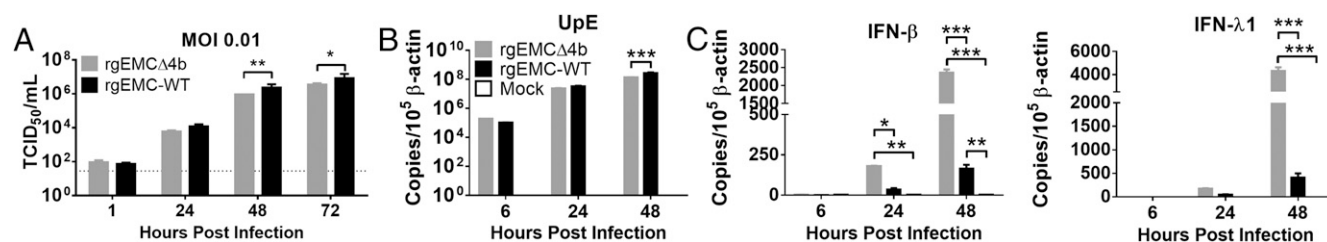


Fig. 4. Comparison of virus replication kinetics and innate immune responses in Calu-3 cells infected with reverse-genetically engineered MERS-CoV, rgEMC-WT, and MERS-CoV with *ORF4b* deletion, rgEMC Δ 4b. (A) Calu-3 cells were infected at an MOI of 0.01. Virus titers in culture supernatants were determined by the TCID₅₀ assay. Means and SEM of three biological replicates are shown. The horizontal dotted line denotes the limit of detection in the TCID₅₀ assay. (B and C) Calu-3 cells were infected at an MOI of 2 with MERS-CoVs rgEMC-WT and rgEMC Δ 4b; mock-infected cells served as negative controls. RNA expression of viral gene UpE (B) and mRNA expression of IFN- β and IFN- λ 1 (C) is shown as the mean and the SEM of three biological replicates. The detection limit of each gene was 20 copies. Each experiment was repeated once, and a representative experiment is shown. Statistical significance was determined by two-way ANOVA with Bonferroni's comparisons: * $P < 0.05$; ** $P < 0.01$; *** $P < 0.001$.

lungs of Ad5-hDPP4-transduced mice and in ex vivo cultures of human bronchus and lung. The mouse model used does not manifest overt clinical disease, and thus a comparison of disease severity was not possible (14). It is notable that the impaired virus replication competence of the West African viruses in human respiratory epithelial cells does not appear to impair the fitness of these viruses in transmitting between dromedaries because these viruses are widespread in camels in West Africa (4, 5, 7).

Because BF785 and Nig1657 differ from EMC and AH13 in having deletions in the *ORF4b* gene, and because the *ORF4b* gene product is reportedly associated with evasion of host cell IFN defense mechanisms (10, 11), we further investigated whether the impaired replication competence correlated with a loss of such immune evasion in Calu-3 cells. In contrast to influenza H5N1, which was a potent inducer of IFN- β , IFN- λ 1, IP10, ISG15, and MX1 by 24 h post infection, the four MERS-CoV had little effect in up-regulating these innate immune responses at 24 h post infection, suggesting that potent innate immune-evasion mechanisms remained active in all four coronaviruses despite the *ORF4b* deletion in BF785 and Nig1657 viruses (Fig. 3). Coronaviruses have multiple antagonists of IFN induction and signaling, and thus deletion of *ORF4b* by itself may not be decisive in this regard. By 48 h post infection, there was detectable induction of innate immune responses by some MERS-CoV, although this was still much lower than those elicited by H5N1 virus. Nig1657 also has deletions in *ORF3*. No consistent pattern was discerned between innate immune responses (or evasion of such responses) and the impaired virus replication competence of BF785 and Nig1657. Taking these findings together, we conclude that the impaired replication phenotype was not associated with the lack of innate immune evasion. In contrast, it was recently reported that a recombinant MERS-CoV clone with *ORF3/4/5* deletions had reduced virus replication competence in Calu-3 (but not Vero) cells and in the lungs of human DPP4-transgenic mice, suggesting that the combined loss of these ORFs does lead to attenuation of the virus (18).

To specifically investigate whether the *ORF4b* deletion contributed to reduced replication competence, we compared recombinant EMC (rgEMC-WT) with an isogenic virus that was deleted in *ORF4b* (rgEMC Δ 4b). We found rgEMC Δ 4b viral titers did not significantly differ from rgEMC-WT at 24 h replication, in contrast with BF785 and Nig1657 viruses where replication was significantly reduced at this time. Thus, the *ORF4b* deletions in BF785 and Nig1657 were likely not major contributors to the reduced virus replication observed in clade C1 virus-infected cells. At 48 h post infection rgEMC-WT replicated to modestly lower titers compared with rgEMC Δ 4b. The rgEMC Δ 4b virus elicited significantly higher mRNA expression of IFN- β , IFN- λ 1, CXCL10 (IP-10), ISG15, and MX1 in rgEMC Δ 4b-infected cells. Previous evidence for an IFN antagonist role for *ORF4b* protein (10, 11) was based solely on the overexpression of *ORF4b*, while our data were generated from an isogenic deletion mutant virus. Increased mRNA of type I

IFN and type III IFN as well as TNF- α suggests that *ORF4b* has effects on IRF-3 as well as NF κ B pathways.

Taken together, our data suggest that BF785 and Nig1657 have reduced replication competence in Calu-3 cells and in ex vivo cultures of human bronchus and lung and, in the case of BF785, also have reduced replication competence in Ad5-hDPP4-transduced mice (comparable experiments were not carried out with Nig1657). Although these viruses have deletions in *ORF4b*, this does not appear to be the major explanation for the reduced viral replication competence of clade C1 viruses. It is relevant that two clade B viruses, Riyadh_1_2012 and Bisha_1_2012, which also have *ORF4b* deletions, have previously been isolated from patients with severe human disease. Thus, *ORF4b* deletions by themselves are unlikely to contribute to altered zoonotic transmission of West African viruses. Furthermore, in previous experiments where EMC virus has been serially passaged in mice to derive mouse-adapted MERS-CoV, such mouse adaptation and increase in virulence for mice have often been associated with deletions or frameshift mutations in all the accessory proteins, including ORF5 (19, 20). Recently, a clade B MERS-CoV with a deletion in *ORF4a* (a different accessory gene) and a minor deletion in *ORF3* has been isolated from humans diagnosed as part of a hospital outbreak in Jordan (21). All 13 viruses from patients sampled during this outbreak had this *ORF4a* deletion, indicating that these viruses were transmissible in humans. *ORF4a* is also known to be an IFN antagonist acting by binding and antagonizing the dsRNA-binding protein PACT (22). It is not yet reported whether *ORF4a* deletions in these human MERS-CoV affect IFN responses or virus replication competence.

Differences in viral genes other than *ORF4b* or *ORF3* genes likely contribute to the impaired viral replication of BF785 and Nig1657. MERS-CoV BF785 and Nig1657 differ from EMC in several proteins, including nsp1, nsp2, nsp3, nsp4, nsp5, nsp6, nsp7, nsp8, nsp12, nsp13, nsl14, nsp15, and nsp16, the spike protein, *ORF3/4/5* gene regions, and N protein (Dataset S2). The spike protein is a crucial determinant of virus tropism and interspecies transmission. However, none of the amino acid differences between Arabian and West African viruses is in the receptor-binding interface.

The observation that *ORF4b*, *ORF4a*, and *ORF3* deletions appear to arise independently in clade B and C viruses and that *ORF4b* deletions are fixed in MERS-CoV from dromedaries West Africa may suggest that the virus is not yet fully adapted to camels and the presence of these genes is either neutral or slightly deleterious to virus growth in these settings. Given the propensity of viruses to discard unnecessary genetic information, these results suggest that these accessory proteins are advantageous in some other reservoir host species, perhaps bats. The time to most recent common ancestor (TMRCA) for MERS-CoV, the >99% nucleotide homology of viruses across a wide geographic area, the genetic instability of the virus in dromedaries, and the lack of endemic infection in dromedaries in parts of the

world (e.g., Kazakhstan) (23) suggest that MERS-CoV has not been endemic in dromedary camels for very long. However, the presence of antibodies to a MERS-CoV-like coronavirus in dromedary sera from Africa and the Middle East collected 30 y ago indicates that the virus has been transmitting in camels for at least this period of time (4). Taken together, these data may suggest that dromedaries, although currently the source of zoonotic infection, are themselves a relatively recent host of MERS-CoV and that the virus is still adapting to this species.

In conclusion, MERS-CoV in Africa are phylogenetically distinct but antigenically similar to those currently circulating in the Arabian Peninsula. Clade C1 MERS-CoV that are enzootic in dromedaries in West Africa had lower replication competence in human respiratory epithelium *in vitro*, in cultures of human bronchus and lung *ex vivo*, and in the lungs of experimentally infected mice. The genetic determinants of this reduced virus replication competence of clade C1 viruses remains to be established. It is possible that these observations may be relevant to explain the apparent lack of zoonotic disease in West Africa. It is important to note that viruses from Egypt were not phenotypically different to those from the Arabian Peninsula, and thus there is no indication that MERS-CoV from East Africa have reduced zoonotic potential. These findings highlight the need for more extensive and sustainable surveillance and monitoring systems, especially in East Africa, including seroepidemiologic studies in humans regularly exposed to dromedaries, to ascertain whether unrecognized zoonotic MERS infections are taking place.

Materials and Methods

Details of the study sites (6, 7), specimen collection, and RT-PCR detection of MERS RNA are detailed in [Supporting Information](#). Representative swab specimens with high MERS-CoV viral load [low threshold cycle (CT) values] were selected for full-length virus genome sequencing, and additional specimens were selected for targeted sequencing of the *ORF3* and *ORF4b* regions ([Supporting Information](#)). Methods used for virus isolation and for the assembly and modification of a full-length BAC cDNA clone to rescue wild-type and mutant recombinant MERS-CoV lacking *ORF4b* are described in [Supporting Information](#).

Phylogenetic Analysis and Phenotypic Comparison of MERS-CoV Isolates. The phylogenetic analysis shown in Fig. 1 was done using the maximum-likelihood

method (PhyML) (24). Other phylogenetic methods are detailed in [Supporting Information](#). Dromedary virus BF785 and Nig1657 viruses isolated as part of this study were chosen for comparison with the prototype human MERS-CoV strain EMC (clade A) provided by R. A. M. Fouchier (Erasmus University Medical Center, Rotterdam, The Netherlands) and a dromedary camel virus, dromedary/Al-Hasa-KFU-HKU13/2013 (AH13) (clade B), isolated in the Kingdom of Saudi Arabia (25). Viruses were isolated and grown in Vero cells, aliquoted, and stored at -80°C until used. The passage history of these viruses is shown in [Dataset S1](#). Antigenic comparison also included dromedary/Egypt NRCE-HKU-270 (15).

Phenotypic comparison of viruses in Calu-3 cells and *ex vivo* cultures of human lung and bronchus were carried out as described in [Supporting Information](#). The procedure for transducing mice with an adenovirus vector expressing human DPP4 has been previously described (14) and is detailed in [Supporting Information](#).

Biosafety and Ethics. Experiments with live MERS-CoV were carried out in biosafety level 3 biocontainment facilities at the University of Hong Kong and the University of Iowa. Studies on the *ex vivo* cultures of human bronchus and lung were approved by the Institutional Review Board of The University of Hong Kong/Hospital Authority Hong Kong West Cluster (UW-13-104). All animal studies were approved by the Institutional Animal Care and Utilization Committee at the University of Iowa.

Statistical Analysis. The statistical analyses are indicated in figure legends and are detailed in [Supporting Information](#). Statistical significance was defined as $P < 0.05$.

ACKNOWLEDGMENTS. We thank Dr. Bart L. Haagmans (Erasmus Medical Centre) for providing a serum (C7) from a dromedary camel immunized with modified vaccinia Ankara vaccine expressing MERS-CoV spike protein and Mr. H. S. Li for excellent technical assistance. The study was supported by research grants from NIH Contract HHSN272201400006C (to M.P. and R.J.W.) and NIH Grant P01 AI060699 (to S.P.), a Commissioned Grant from the Health and Medical Research Fund, Food and Health Bureau, Government of the Hong Kong Special Administrative Region (to M.P.), and Deutsche Forschungsgemeinschaft Grant DR772/12-1 (to C.D.). A.R. is funded by The Wellcome Trust Grant 206298, and G.D. is supported by a Mahan Postdoctoral Fellowship from the Fred Hutchinson Cancer Research Center. The research funders had no role in the design, data collection, and interpretation or the decision to submit this work for publication.

- World Health Organization (December 5, 2016) WHO MERS-CoV Global Summary and risk assessment. Available at www.who.int/emergencies/mers-cov/mers-summary-2016.pdf?ua=1. Accessed February 18, 2018.
- Al-Tawfiq JA, Perl TM (2015) Middle East respiratory syndrome coronavirus in healthcare settings. *Curr Opin Infect Dis* 28:392–396.
- Haagmans BL, et al. (2014) Middle East respiratory syndrome coronavirus in dromedary camels: An outbreak investigation. *Lancet Infect Dis* 14:140–145.
- Reusken CB, Raj VS, Koopmans MP, Haagmans BL (2016) Cross host transmission in the emergence of MERS coronavirus. *Curr Opin Virol* 16:55–62.
- Chu DK, et al. (2014) MERS coronaviruses in dromedary camels, Egypt. *Emerg Infect Dis* 20:1049–1053.
- Chu DK, et al. (2015) Middle East respiratory syndrome coronavirus (MERS-CoV) in dromedary camels in Nigeria, 2015. *Euro Surveill* 20, 10.2807/1560-7917.ES.2015.20.49.30086.
- Miguel E, et al. (2017) Risk factors for MERS coronavirus infection in dromedary camels in Burkina Faso, Ethiopia, and Morocco, 2015. *Euro Surveill* 22:30498.
- Ithete NL, et al. (2013) Close relative of human Middle East respiratory syndrome coronavirus in bat, South Africa. *Emerg Infect Dis* 19:1697–1699.
- Thornbrough JM, et al. (2016) Middle East respiratory syndrome coronavirus NS4b protein inhibits host RNase L activation. *MBio* 7:e00258-16.
- Yang Y, et al. (2015) Middle East respiratory syndrome coronavirus ORF4b protein inhibits type I interferon production through both cytoplasmic and nuclear targets. *Sci Rep* 5:17554.
- Matthews KL, Coleman CM, van der Meer Y, Snijder EJ, Frieman MB (2014) The ORF4b-encoded accessory proteins of Middle East respiratory syndrome coronavirus and two related bat coronaviruses localize to the nucleus and inhibit innate immune signalling. *J Gen Virol* 95:874–882.
- Scobey T, et al. (2013) Reverse genetics with a full-length infectious cDNA of the Middle East respiratory syndrome coronavirus. *Proc Natl Acad Sci USA* 110:16157–16162.
- Haagmans BL, et al. (2016) An orthopoxvirus-based vaccine reduces virus excretion after MERS-CoV infection in dromedary camels. *Science* 351:77–81.
- Zhao J, et al. (2014) Rapid generation of a mouse model for Middle East respiratory syndrome. *Proc Natl Acad Sci USA* 111:4970–4975.
- Chan RW, et al. (2014) Tropism and replication of Middle East respiratory syndrome coronavirus from dromedary camels in the human respiratory tract: An *in-vitro* and *ex-vivo* study. *Lancet Respir Med* 2:813–822.
- Zielecki F, et al. (2013) Human cell tropism and innate immune system interactions of human respiratory coronavirus EMC compared to those of severe acute respiratory syndrome coronavirus. *J Virol* 87:5300–5304.
- Faye B (2013) Camel meat in the world. *Camel Meat and Meat Products*, eds Kadim I, Maghoub O, Faye B, Farouk M (CAB International, Oxfordshire, UK), pp 7–16.
- Menachery VD, et al. (2017) MERS-CoV accessory ORFs play key role for infection and pathogenesis. *MBio* 8:e00665-17.
- Cockrell AS, et al. (2016) A mouse model for MERS coronavirus-induced acute respiratory distress syndrome. *Nat Microbiol* 2:16226.
- Li K, et al. (2017) Mouse-adapted MERS coronavirus causes lethal lung disease in human DPP4 knockin mice. *Proc Natl Acad Sci USA* 114:E3119–E3128.
- Lamers MM, et al. (2016) Deletion variants of Middle East respiratory syndrome coronavirus from humans, Jordan, 2015. *Emerg Infect Dis* 22:716–719.
- Siu KL, et al. (2014) Middle East respiratory syndrome coronavirus 4a protein is a double-stranded RNA-binding protein that suppresses PACT-induced activation of RIG-I and MDA5 in the innate antiviral response. *J Virol* 88:4866–4876.
- Miguel E, et al. (2016) Absence of Middle East respiratory syndrome coronavirus in camels, Kazakhstan, 2015. *Emerg Infect Dis* 22:555–557.
- Guindon S, et al. (2010) New algorithms and methods to estimate maximum-likelihood phylogenies: Assessing the performance of PhyML 3.0. *Syst Biol* 59:307–321.
- Hemida MG, et al. (2014) MERS coronavirus in dromedary camel herd, Saudi Arabia. *Emerg Infect Dis* 20:1231–1234.